



Contents lists available at ScienceDirect

# International Journal of Applied Earth Observations and Geoinformation

journal homepage: [www.elsevier.com/locate/jag](http://www.elsevier.com/locate/jag)

## Phenological and physiological responses of the terrestrial ecosystem to the 2019 drought event in Southwest China: Insights from satellite measurements and the SSiB2 model

Lingfeng Li<sup>a</sup>, Bo Qiu<sup>a,\*</sup>, Weidong Guo<sup>a</sup>, Yiping Zhang<sup>b</sup>, Qinghai Song<sup>b</sup>, Jiuyi Chen<sup>a</sup><sup>a</sup> School of Atmospheric Sciences, and Joint International Research Laboratory of Atmospheric and Earth System Sciences, Nanjing University, 210023 Nanjing, China<sup>b</sup> CAS Key Laboratory of Tropical Forest Ecology, Xishuangbanna Tropical Botanical Garden, Chinese Academy of Sciences, 666303 Mengla, China

## ARTICLE INFO

## Keywords:

Drought  
Plant physiological response  
Solar-induced chlorophyll fluorescence  
Water stress

## ABSTRACT

Understanding plant phenological and physiological changes in response to drought will provide key insight into the response of terrestrial ecosystems to climate change, but is still limited due to the increased drought severity and frequency in recent decades. Here, we combine solar-induced chlorophyll fluorescence (SIF) along with SSiB2 (Simplified Simple Biosphere Model) simulations to investigate the plant phenological and physiological responses to the 2019 drought in southwestern China. Our results show that this 2019 drought had substantial impacts on vegetation phenology and photosynthesis due to the soil moisture deficit in spring, while the rewatering process in July alleviated the water deficit and reduced drought damage to plants. Moreover, SIF observations provide a physiology-related vegetation response, as the recovery of plant photosynthesis indicated by fluorescence yield (SIF<sub>yield</sub>) is much stronger than the recovery of greenness described by vegetation indices during the rewatering in July. The SSiB2 simulations captured the physiological response of plants to moisture deficit during drought period, while the lack of realistic energy dissipation mechanisms under stressed conditions may lead to discrepancies in the timing of peak response to drought. Our findings highlight the prospective application of remote sensing SIF measurements in monitoring the timely response of plant physiology to changes in water conditions and to provide important information for model evaluation and improvement.

### 1. Introduction

Terrestrial ecosystems serve as a key factor influencing carbon dioxide concentrations in the atmosphere (Humphrey et al., 2021). More than 30% of anthropogenic CO<sub>2</sub> emissions are absorbed by terrestrial ecosystems, which effectively mitigates global warming (Friedlingstein et al., 2019). However, accumulating evidence shows that anthropogenic climate warming will increase extreme weather and climate events (Stocker, 2014). Among extreme climatic events, droughts and heatwaves are expected to aggravate water stress through increased deficits of precipitation and soil moisture (De Kauwe et al., 2019) and thus have substantial impacts on vegetation by impairing photosynthesis as well as triggering tree mortality and crop failure (Beillouin et al., 2020), thereby impairing the carbon absorption capacity of terrestrial ecosystems (Smith et al., 2020).

One of the largest terrestrial carbon sinks in China lies in the southwestern regions (Piao et al., 2009). Being widely covered by

subtropical vegetation, a strong carbon sequestration capacity is found year round (Wang et al., 2020). In recent decades, climate extremes such as drought events in the Southwest China region have shown increasing severity and frequency (Han et al., 2014) and have adversely affected vegetation phenology and photosynthesis in the region (Wang et al., 2019). For example, a prolonged and spatially widespread extreme drought event occurred from autumn 2009 to spring 2010 (Li et al., 2019) and substantially suppressed plant photosynthesis, resulting in a significant GPP (gross primary productivity) loss. Overall, plant photosynthesis is vulnerable to frequent drought suppression in Southwest China.

Recently, solar-induced fluorescence (SIF) has revealed a novel approach for detecting vegetation photosynthesis (Frankenberg et al., 2011). Being directly related to the photochemical process, SIF enables accurate and timely monitoring of the physiologically relevant responses of vegetation to extreme climate events (Sun et al., 2018). Evidence from observations indicates the promising applications of SIF

\* Corresponding author.

E-mail address: [qiubo@nju.edu.cn](mailto:qiubo@nju.edu.cn) (B. Qiu).<https://doi.org/10.1016/j.jag.2022.102832>

Received 4 March 2022; Received in revised form 27 April 2022; Accepted 19 May 2022

Available online 27 May 2022

1569-8432/© 2022 The Authors. Published by Elsevier B.V. This is an open access article under the CC BY-NC-ND license (<http://creativecommons.org/licenses/by-nc-nd/4.0/>).

observations in investigating the response of plant phenology and photosynthesis to extreme drought events at various timescales (Jiao et al., 2019). Moreover, satellite SIF retrieval has provided promising information for constraining photosynthesis progress simulations in land surface models. During the last decade, substantial improvements have been achieved in the development of mechanistic SIF schemes (Qiu et al., 2019a). However, studies focusing on vegetation responses to drought by combining remotely sensed measurements along with model simulations are still very rare.

Here, we combine remotely sensed observations together with simulations from the terrestrial biosphere model to investigate the plant phenological and physiological responses to the 2019 drought in Yunnan Province, China. We use satellite observations from various sources along with the SSiB2 (Simplified Simple Biosphere Model) coupled with the SIF scheme to examine the plant phenology and physiology response to the extreme drought event in 2019. Based on the observations and model simulations, we aim to (1) examine the effects of the 2019 drought on plant phenology and physiology and the underlying mechanisms of vegetation to drought dynamics; and (2) assess the capability of the land surface model in reproducing the plant responses to water deficits during a severe drought event.

## 2. Materials and methodology

### 2.1. Meteorological variables and soil water content

The China Meteorological Administration provides daily mean temperature and daily precipitation data. We performed quality control and discarded sites with missing values exceeding 1% of the total number of days. As a result, data from 24 meteorological stations within Yunnan Province remain. We also collected the 36 km × 36 km Soil Moisture Active Passive (SMAP) level-3 soil moisture product (SPL3SMP version 8) and the 0.25° European Space Agency Climate Change Initiative (ESA CCI) soil moisture dataset (version 05.2). Both data have shown great consistency as compared with in situ measurements (Dorigo et al., 2017; O'neill et al., 2019). Data from 2015 to 2019 are used in this study.

### 2.2. Remotely sensed vegetation indices and SIF measurements

The Orbiting Carbon Observatory 2 (OCO-2) is a high-precision observation satellite flying in a sun-synchronous orbit, providing robust and accurate SIF retrieval due to its high spectral resolution. We collected OCO-2 Level 2 bias-corrected SIF (OCO2\_L2\_Lite\_SIF V10r) observations from GES DISC (Gunson, 2020), and processed the original daily SIF at 757 nm from 2015 to 2019 into gridded monthly data with a 1° spatial resolution. In addition to the OCO-2, the Tropospheric Monitoring Instrument (TROPOMI) is a sun-synchronous satellite providing nearly daily global coverage at a high spatial resolution due to its wide swath width (~2600 km) as compared to OCO-2 (~10 km) (Köhler et al., 2018). TROPOMI SIF from February 2018 to December 2019 is also used in this study.

As the SIF value depends largely on the magnitude of photosynthetically active radiation (PAR), we collected the 1° × 1° monthly PAR (SYN1deg Ed4.1) data from CERES (Doelling et al., 2016). We summed the surface PAR direct flux and the diffuse flux for all-sky conditions as the total amount of PAR flux. In addition, the fraction of PAR (fPAR) product from MODIS (MOD15A2H Version 6) was collected from the LP DAAC (Myneni et al., 2015). The 8-day fPAR dataset with a 500-meter pixel size is aggregated to 1° × 1° monthly data to maintain consistency with the spatiotemporal resolution of SIF.

The remote sensing normalized difference vegetation index (NDVI) and enhanced vegetation index (EVI) are recognized as important vegetation phenological indicators. In this study, we obtained the MODIS 0.05° × 0.05° product (MOD13C2 Version 6) from LP DAAC

(Didan, 2015) and aggregated it to monthly data with 1° × 1° spatial resolution. Data from 2015 to 2019 are used in this study. Documentation and detailed descriptions can also be found at the MODIS and LP DAAC websites.

### 2.3. In situ observations

The ChinaFlux of Xishuangbanna Tropical Rainforest Ecosystem Flux Observation Station (XSBN) (21°55'39" N, 101°15'55" E) sits in southwestern Yunnan Province, China. In this study, ground-based measurements of XSBN from 2015 to 2019 provide additional validating information for investigating drought dynamics as well as drought effects on vegetation phenology and physiology. We derived the canopy top air temperature, precipitation, PAR, and other meteorological variables, as well as the GPP of flux observations, and calculated the light-use efficiency of vegetation as an important supplement to explore the physiological response of plants under drought stress. Further details on the geography, climate, soil properties, and vegetation of this site and nearby region are listed in previous studies (Fei et al., 2019).

### 2.4. SSiB2 model

The SSiB2 model coupled with the SIF module was used in this study. SSiB2 realistically and efficiently simulates complex biophysical processes and provides accurate descriptions of the surface energy partition and vegetation canopy processes (Zhan et al., 2003). Recently, the SIF module considering the mechanisms of chlorophyll fluorescence was incorporated into SSiB2, which enables the SSiB2 model to reproduce global patterns of SIF measured from satellites (Qiu et al., 2018).

In this study, we obtained the atmospheric forcing variables from the ERA5-Land dataset to drive the SSiB2 model offline (Muñoz Sabater, 2019). The 3-hourly forcing data were aggregated to 1° × 1° to match the spatial resolution of the observations. Since the leaf area index (LAI) plays a crucial role in SIF modeling as the key information to characterize canopy structure, we obtained the 8-day GLASS LAI dataset (LAI MODIS 0.05°, Version V60) and aggregated it to 1° × 1° monthly data (Liang et al., 2021). The model takes the 4-year average monthly LAI from 2015 to 2018 as input parameters throughout the entire period of simulation to provide information on the seasonal variations in LAI. We processed an offline run of SSiB2 with an integration time step of 3 h and a spatial resolution of 1°. The simulation period starts from January 2013 and ends in December 2019. Simulations of the first two years are used as the spin-up time, and the results from 2015 to 2019 are analyzed and discussed in this paper.

### 2.5. Data analysis

According to Guanter et al. (2014), the intensity of solar radiation directly affects the values of GPP and SIF to a large extent. By using PAR and fPAR to normalize SIF and GPP, we derived the light-use efficiency (LUE) as well as SIF<sub>PAR</sub> and SIF<sub>yield</sub>, which can be formulated as follows:

$$\text{LUE} = \text{GPP}/\text{APAR} = \text{GPP}/(\text{PAR} \times \text{fPAR}) \quad (1)$$

$$\text{SIF}_{\text{PAR}} = \text{SIF}/\text{PAR} \quad (2)$$

$$\text{SIF}_{\text{yield}} = \text{SIF}/\text{APAR} = \text{SIF}/(\text{PAR} \times \text{fPAR}) \quad (3)$$

By dividing by PAR and APAR, LUE eliminates the influence of APAR on GPP, and SIF<sub>PAR</sub> and SIF<sub>yield</sub> eliminate the influence of PAR and APAR on SIF. During drought and heatwaves, PAR and APAR are expected to rise above normal levels. Therefore, these variables can be used as indicators of vegetation photosynthesis efficiency, which can contribute to our understanding of the physiological response of drought stressed plants.

To obtain the drought stress-forced signals and vegetation response dynamics, we calculated the standardized anomalies for the aforementioned

tioned meteorological variables as well as the vegetation phenological and physiological indicators. The pixel-by-pixel standardized anomalies can be formulated as follows:

$$STDA_{2019} = (VAR_{2019} - AVG_{2015-2018})/SD_{2015-2018} \quad (4)$$

where  $STDA_{2019}$  is the standardized anomaly of a variable in 2019,  $VAR_{2019}$  is the value of the same variable in 2019, and  $AVG_{2015-2018}$  and  $SD_{2015-2018}$  are the average values and standard deviations from 2015 to 2018.

### 3. Results

#### 3.1. A "natural rewatering" during a severe drought in 2019

According to the meteorological data, a severe and persistent drought event occurred in Yunnan in the spring of 2019 (Fig. 1) and continued throughout the summer. The temperature from April to June is approximately 1.4 °C above the multiyear average. From April to

September, the air temperature at more than 80% of the sites exceeded the multiyear average by 1 standard deviation (SD), while the precipitation in nearly 60% of the areas was below -1 SD (Fig. 1a and b). Severe meteorological drought has led to a soil moisture deficit, resulting in 10% and 5% deficits in SMAP and ESA CCI soil moisture, respectively. In terms of spatial distribution, approximately 94% and 89% of the region has an anomaly below -1 SD for SMAP and ESA CCI soil moisture, respectively (Fig. 1c and d). In summary, most of the Yunnan region experienced strong and persistent hydrological drought in 2019 as revealed by the spatial patterns of precipitation and soil water content (SWC).

The seasonal cycles of temperature, precipitation, and SWC in 2019 and the multiyear mean are shown in Fig. 2. Overall, high temperature, low precipitation, and strong soil moisture deficit dominated the spring and summer of 2019, as significance was regarded as a departure >1 SD. In April, May, June, and August 2019, the regional average precipitation and soil moisture in Yunnan were both lower than -1 SD, while the temperature was higher than 1 SD (Fig. 2). From April to June, the air temperature anomalies all exceeded 1 °C, and the precipitation was

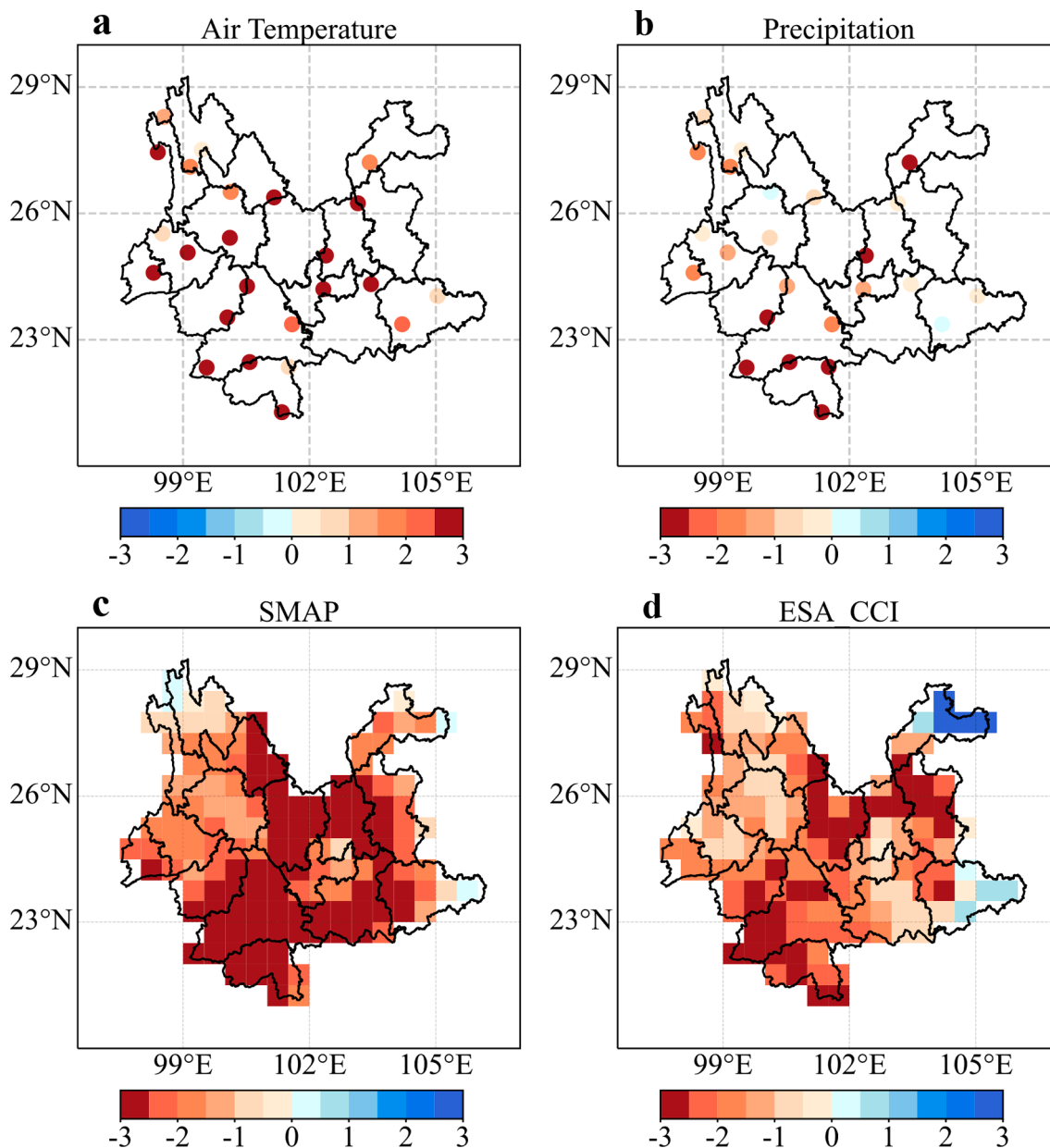


Fig. 1. Standardized anomalies of (a) temperature, (b) precipitation, (c) SMAP SWC, and (d) ESA CCI SWC from April to September 2019.

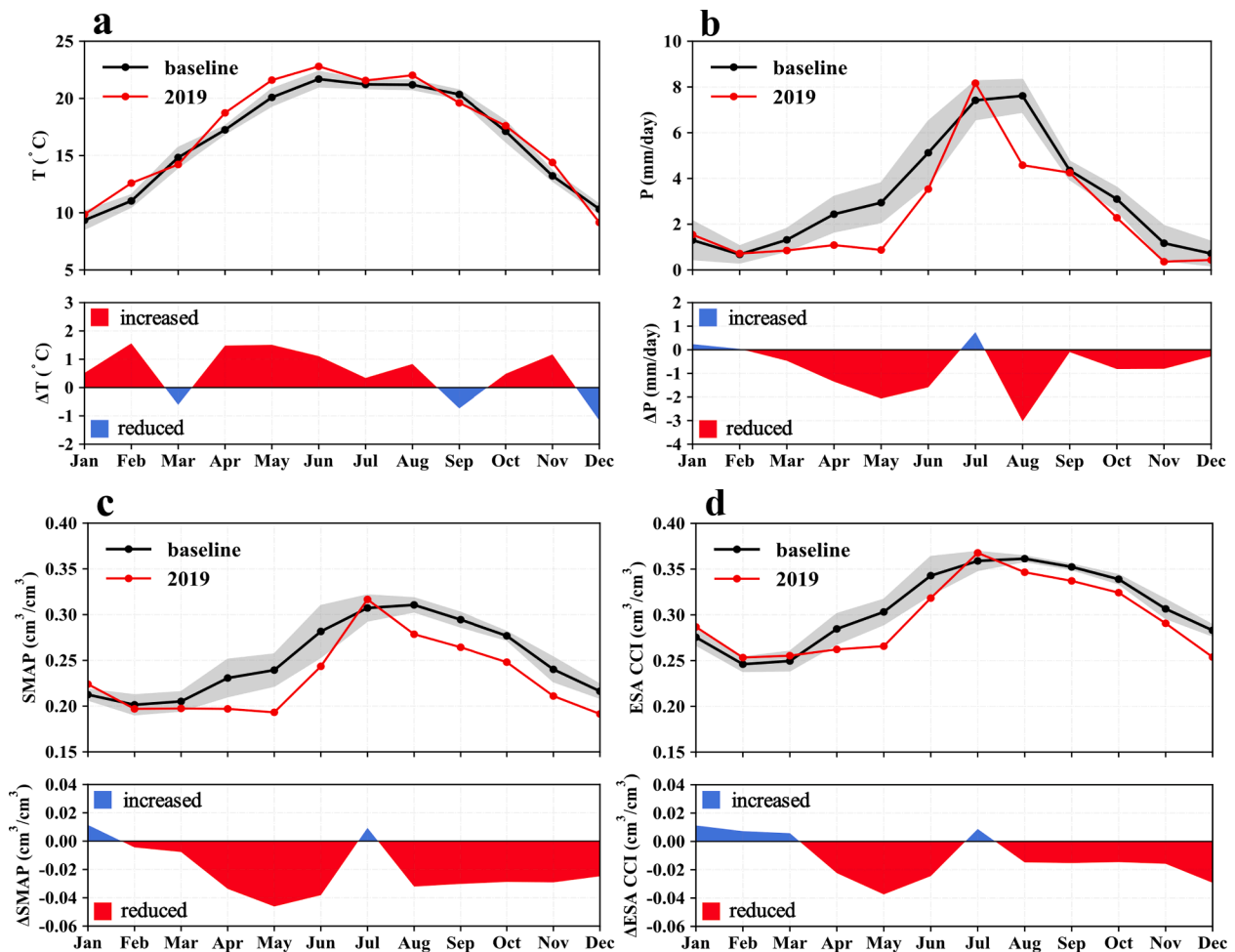


Fig. 2. Seasonal variations and the 2019 anomaly of (a) temperature, (b) precipitation, (c) SMAP SWC, and (d) ESA CCI SWC. The black curves show the multiyear average from 2015 to 2018 and the red curves show the drought year (2019) values. The gray shaded areas indicate the range of one standard deviation around the multiyear average.

approximately 50% less than the multiyear average. However, the precipitation significantly increased in July, which replenished the soil water and led to a positive soil moisture anomaly. This special drought dynamic can be considered a natural “rewatering” process, which is defined as a significant alleviation of soil water shortage during or after a severe drought event. The “rewatering” experiment is usually conducted at the site level or for specified vegetation types to investigate the rate and degree of photosynthetic recovery of drought stressed plants after rewatering treatment (Chen et al., 2016; Zhong et al., 2019). The 2019 drought dynamic in Yunnan is characterized by a persistent drought from spring to early summer, followed by a significant relief of water shortage in July, and thus, it can be considered a natural rewatering process at the regional scale, which provides ideal conditions for understanding the physiological response of plant resilience to water supply during a severe drought.

### 3.2. Satellite-observed phenological and physiological suppression and recovery processes

The 2019 drought in Yunnan is characterized by precipitation and soil moisture deficits from spring to autumn, while abundant precipitation alleviates water stress in July. Overall, the 2019 drought in Yunnan altered the vegetation phenology due to the large water deficit in the early stage of the growing season, as significant negative anomalies of vegetation growth and physiology from April to June are widely distributed in the Yunnan region (Fig. S1). The seasonal cycles of

vegetation indices (VIs) and SIF are shown in Fig. 3. As the moisture stress strengthens, the growth of vegetation has slowed since April. The EVI, NDVI, and OCO-2 SIF in May and June were all significantly below the multiyear averages. In particular, the trend in SIF turns from upward to downward in April and May, indicating the severe adverse impacts of drought on vegetation photosynthesis, while such a downward trend could not be captured by VIs. In July, both VIs and SIF recovered rapidly in response to the rewatering process. The vegetation restoration demonstrated by VIs is stronger than that of SIF. In August, both the EVI and NDVI have higher values than the multiyear average, while the OCO-2 SIF merely rises to multiyear average levels. Limited by the short observation period since 2018, the monthly TROPOMI SIF from 2018 to 2019 is shown in Fig. 3d. The comparison of OCO-2 and TROPOMI SIF from 2018 to 2019 is also shown in Fig. S2. Although derived from different sources, both TROPOMI and OCO-2 SIF respond to changes in moisture conditions in a timely manner by exhibiting a consistent downward trend from April to May as well as a recovery process after rewatering, indicating the capability of remotely sensed SIF data to sensitively characterize the plant photosynthetic response to water stress.

Fig. 4 shows the seasonal cycle of the effective yield of fluorescence ( $SIF_{PAR}$  and  $SIF_{yield}$ ). Similar to VIs and SIF, the fluorescence yield shows significant negative anomalies during the spring and early summer of 2019. The  $SIF_{PAR}$  in May and June is approximately 20% lower than the multiyear average, while  $SIF_{yield}$  from April to June is reduced by approximately 30% and has an anomaly below  $-1$  SD. With the sharp

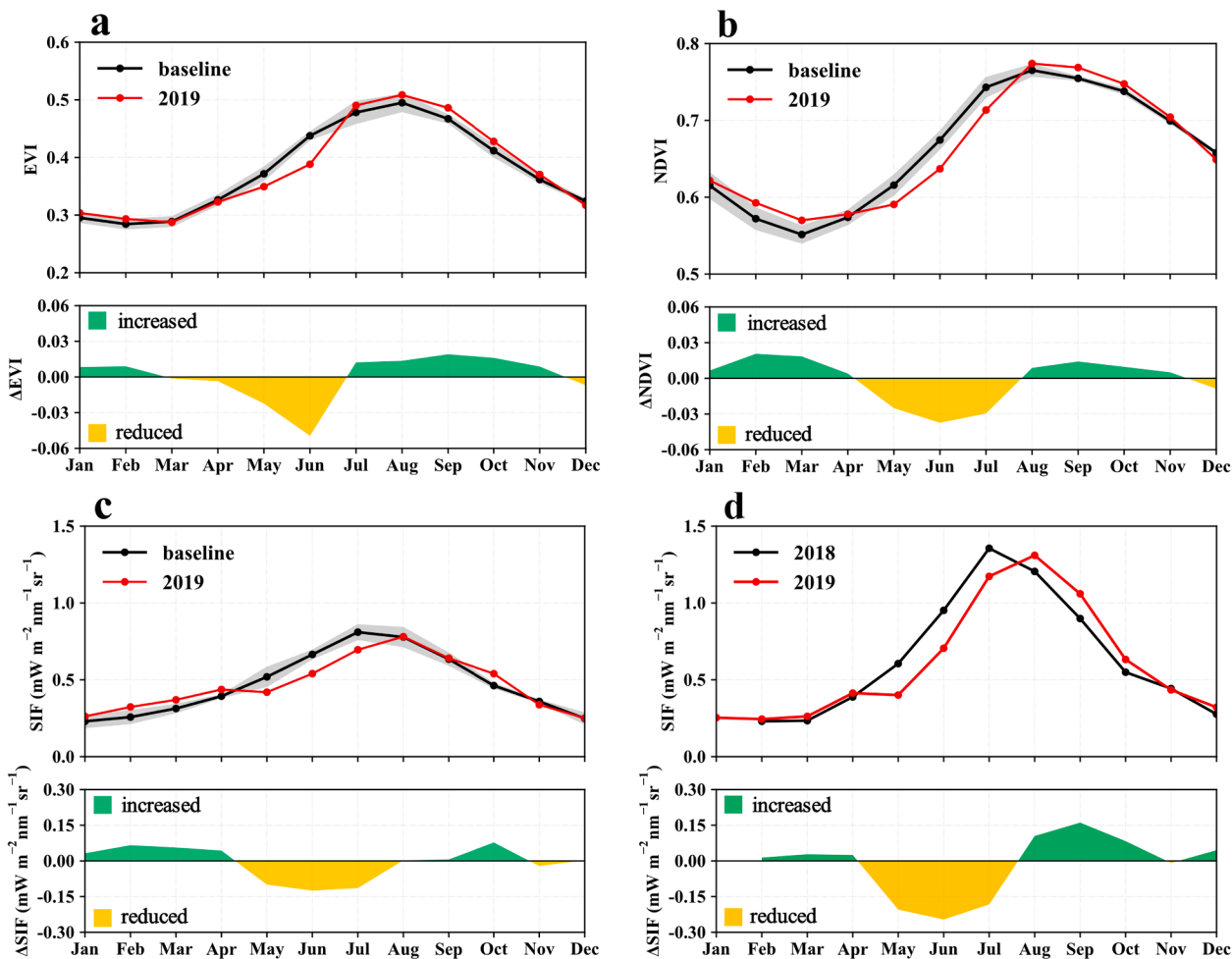


Fig. 3. Seasonal variations and the 2019 anomaly of (a) EVI, (b) NDVI, (c) OCO-2 SIF, and (d) TROPOMI SIF in Yunnan. The black curves of (a), (b), and (c) represent the monthly multiyear mean values from 2015 to 2018, while the black curve of (d) shows the 2018 values of TROPOMI SIF; the red curves show the drought year (2019) values. The gray shaded areas indicate the range of one standard deviation around the multiyear average.

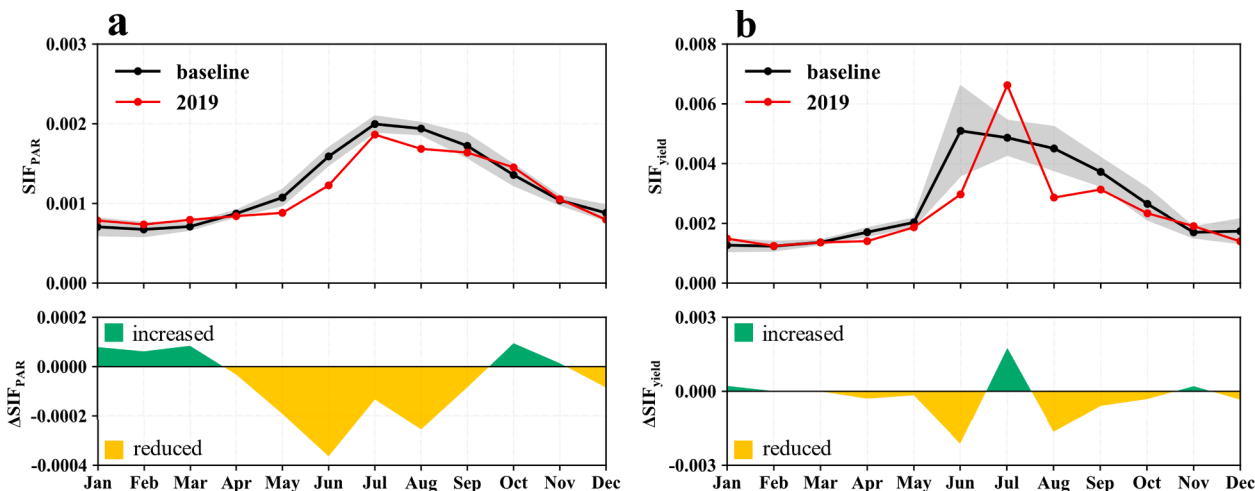


Fig. 4. Seasonal variations and the 2019 anomaly of OCO-2 (a)  $SIF_{PAR}$  and (b)  $SIF_{yield}$  in Yunnan. The black curves show the averages from 2015 to 2018 and the red curves show the drought year (2019) values. The gray shaded areas indicate the range of one standard deviation around the multiyear average.

increases in precipitation and soil moisture in July, both  $SIF_{PAR}$  and  $SIF_{yield}$  recover rapidly. In July,  $SIF_{yield}$  significantly exceeds the multi-year average, followed by a sharp decline in August and September, which is consistent with the water condition. The seasonal cycles of

precipitation and LUE derived from XSBN are shown in Fig. 5. Similar to the  $SIF_{yield}$ , the LUE maintained a continuous downward trend since March due to the persistent rainfall deficit in spring and rose rapidly when rewatering occurred in July. Overall, the results from satellite

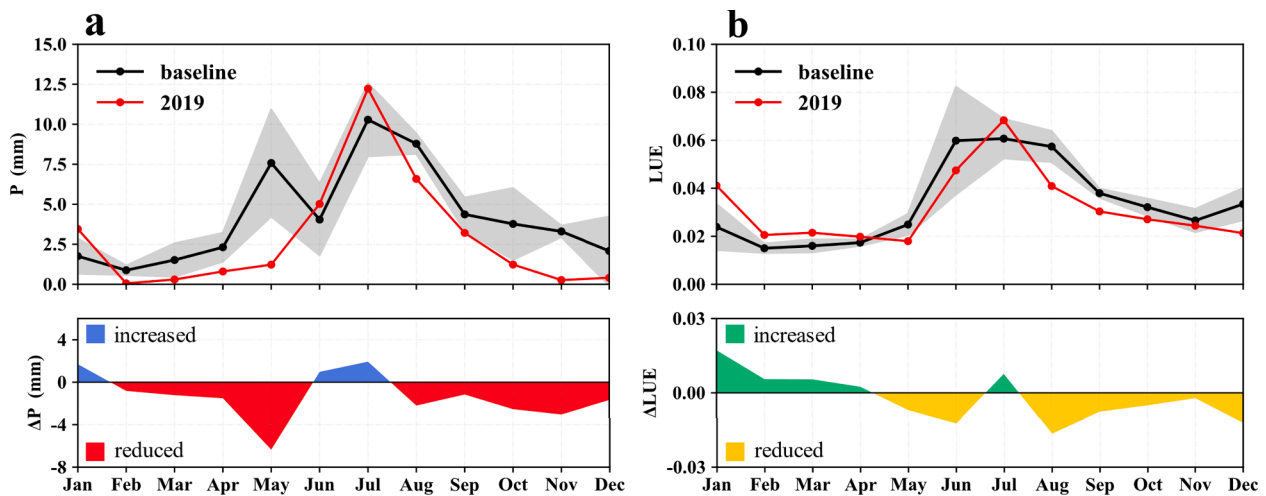


Fig. 5. Seasonal variations and the 2019 anomaly of (a) precipitation and (b) LUE of XSBN. The black curves represent the multiyear average from 2015 to 2018 and the red curves show the drought year (2019) values. The gray shaded areas indicate the range of one standard deviation around the multiyear average.

retrievals indicate that SIF and SIF-related variables, especially  $SIF_{yield}$ , have an accurate and timely response to the rapid changes in moisture conditions during the 2019 drought process. The response of LUE to water stress agrees well with  $SIF_{yield}$ , indicating the high sensitivity and the capability of  $SIF_{yield}$  in capturing plant physiological responses to water condition changes.

### 3.3. Model-simulated phenological and physiological responses

In addition to the timely and accurate phenological and physiological responses captured by remote sensing and in situ observations, we simulated the photosynthetic response of vegetation using SSiB2 coupled with the SIF module. The evaluation of SSiB2 using OCO-2 measurements is shown in Fig. S3. In general, the simulated SIF agrees with the OCO-2 observations in the spatial distribution as well as seasonal cycles. The four-year average of SIF simulations from 2015 to 2018 shows relatively consistent spatial distributions with the OCO-2 measurements, as large values of SIF are centered in the southwestern region of Yunnan. The seasonality of simulated SIF agrees reasonably well with OCO-2, although discrepancies such as the lower values of SSiB2 simulations during the growing season still exist. Overall, the seasonal cycle and the spatial distribution of the four-year average SIF simulations are consistent with the OCO-2 observations, with a spatial correlation coefficient of 0.79, indicating a reasonable capability of SSiB2 in

simulating SIF in the Yunnan region.

Fig. 6 shows the seasonal cycles of the simulated SIF,  $SIF_{yield}$ , GPP, and LUE anomalies averaged in Yunnan Province. Similar to the OCO-2 observations, the simulated SIF and  $SIF_{yield}$  were severely suppressed by drought since spring and rapidly recovered during the rewatering process. The simulated GPP also shows negative anomalies in the spring and early summer of 2019, with an average decline of nearly 40% from April to June, and the seasonal cycle of the LUE anomaly agrees well with  $SIF_{yield}$ . However, the simulated SIF is generally numerically smaller than the OCO-2 observations. In terms of indicating the response to drought, the largest negative anomaly of the SSiB2 SIF appears in May, while that of the OCO-2 SIF appears in June. Overall, the SSiB2 incorporated with the SIF module reproduces the majority of the physiological responses to drought dynamics, while discrepancies such as the timing of the peak response to drought still exist.

## 4. Discussion

### 4.1. Prospective application of SIF to detect plant physiological changes due to water deficit

Evidence from ground and satellite-based observations has indicated higher sensitivities of SIF to drought and heatwaves than traditional VIs, as SIF can directly reflect the photosynthetic activity of vegetation (Qiu

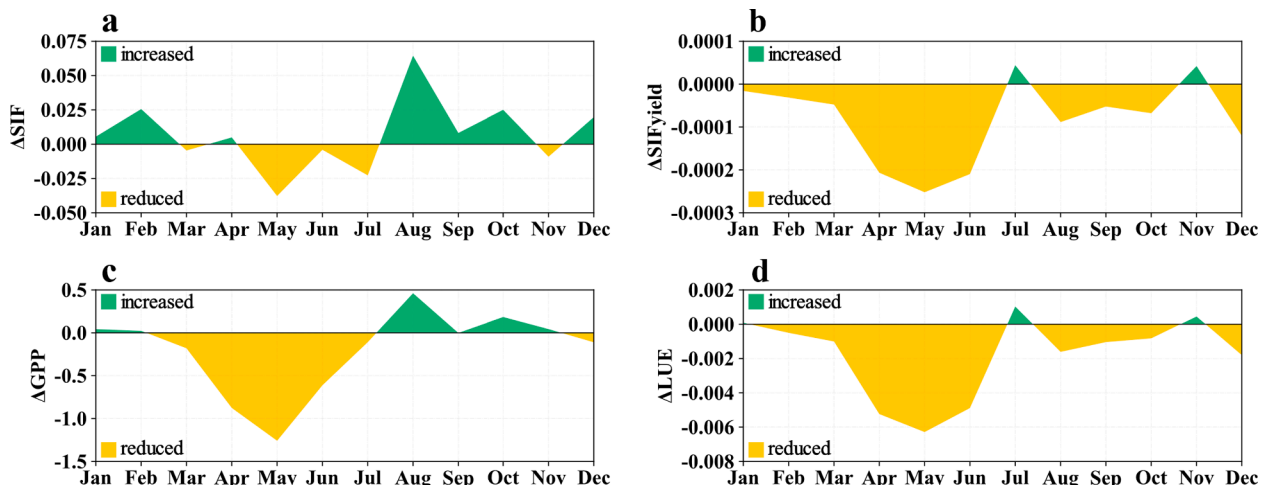


Fig. 6. Regional anomalies in 2019 for the SSiB2 simulated (a) SIF, (b)  $SIF_{yield}$ , (c) GPP, and (d) LUE of Yunnan.

et al., 2020). Remotely sensed SIF measurements have exhibited accurate and timely responses to external moisture and thermal stresses for various plant functional types (Yoshida et al., 2015). Most of the studies focus on capturing the timely response to moisture deficits at the beginning of the drought with SIF data (Song et al., 2018), while our study uses SIF measurements to investigate the recovery of vegetation from drought or the rewatering effects on plant photosynthesis during the drought period.

The results of remotely sensed observations indicate that the fluorescence yield of SIF is more sensitive to changes in water conditions than vegetation greenness. With the onset and intensification of drought from April to June, both SIF and VIs have sharp reductions due to the persistent depletion of soil moisture. However, during the rewatering period in July when precipitation and soil moisture rise above normal levels, SIF<sub>yield</sub> increases sharply above normal in response to abundant precipitation, while the VIs indicate the restoration of vegetation through a smaller negative anomaly. According to previous drought treatments and rewatering experiments at the site level, drought-induced suppression of vegetation growth and photosynthetic activities can be significantly recovered after rewatering (Efeoğlu et al., 2009; Zhong et al., 2019). Therefore, the contradiction between VIs and SIF<sub>yield</sub> in describing the resilience of vegetation to rewatering reflects the limitations of greenness-based VIs for describing the physiological state of vegetation and the response to water stress. After the rewatering period, SIF<sub>yield</sub> drops below the normal level due to the soil moisture deficit, while the VIs remain larger than the multiyear average since August. Combining the comparisons of SIF-related variables and VIs during the drought and rewatering periods, SIF observations, especially the fluorescence yield, are more sensitive to soil moisture changes than traditional VIs. Moreover, as the response of vegetation photosynthesis to environmental stress can also be captured by LUE (Yang et al., 2015), close relationships between SIF<sub>yield</sub> and LUE are found among different vegetation types (Li et al., 2020). Our results also reveal an agreement between SIF<sub>yield</sub> and LUE in capturing plant physiological responses to severe moisture deficits as well as the rewatering process (Figs. 4 and 5). The consistency of SIF<sub>yield</sub> and LUE provides evidence that remotely sensed SIF has a high sensitivity to water stress. Our results highlight the applications of SIF observations in assessing the resistance and resilience of photosynthetic activities.

#### 4.2. Uncertainties and limitations

Advances in satellite SIF observations have provided novel approaches for evaluating and improving the simulation of photosynthetic processes in land surface models. Process-based models coupled with SIF schemes can provide an estimation of the photosynthetic responses to water condition changes (Qiu et al., 2019b). According to the simulations from SSiB2, GPP and SIF exhibit suppression from May to July and recover after the rewatering process, which is consistent with the remotely sensed measurements. The simulated SIF<sub>yield</sub> and LUE also decreased during the spring of 2019 and significantly increased in July due to the water supply (Fig. 6). This result indicates that the physiological responses of vegetation to this drought can be reasonably reproduced by the SSiB2 model.

Although most of the vegetation responses to the 2019 drought in Yunnan can be captured by the model, some disagreements with satellite observations can be found in this case. The OCO-2 SIF<sub>yield</sub> has the largest reductions in June compared to the multiyear mean, while the SSiB2 model shows modest reductions in June (Figs. 4 and 6). The model bias may be caused by the energy dissipation process during the drought period. Previous studies have shown that nonphotochemical quenching (NPQ), a protective mechanism employed by plants to emit energy in the form of heat, is critical to the dissipation of excessive solar radiation when experiencing external stress (Lee et al., 2015). Recently, a plant protection mechanism to dissipate heat stress and intensify solar

radiation by largely increasing NPQ was found by Martini et al. (2022). NPQ tends to be saturated during the heatwave period, which changes the energy dissipation distributions and thus affects the SIF value. However, this mechanism is not well described in the SIF model. Fluorescence parameterization, which is widely used in some terrestrial biosphere models (Parazoo et al., 2020), was developed from the link between the photosynthetic light saturation process and NPQ (Magney et al., 2020). The poor characterization of NPQ saturation during high light and heat stress may result in SIF bias in the models. The simulated SIF<sub>yield</sub> from the SSiB2 model tends to have less reduction in June compared to the satellite-based SIF<sub>yield</sub>, indicating the model bias in simulating the allocation of energy dissipation pathways toward SIF during extreme events. In the future, more fluorescence and NPQ observations can be used to constrain the fluorescence parameterization, thereby improving the model performance in simulating SIF under extreme conditions.

#### 5. Conclusion

In this paper, we investigate the impacts of extreme drought on the photosynthetic activity of subtropical ecosystems in Yunnan. Two satellite SIF observations and simulations from the SSiB2 model are used to improve the understanding of drought damage on plant physiology and the resilience of photosynthesis after rewatering. There is a natural rewatering process during the continuous severe drought from April to September. During drought, both the simulated and observed SIFs exhibited significant reductions during drought, while discrepancies existed in the timing of the peak response to drought. Furthermore, SIF<sub>yield</sub> shows higher sensitivity to moisture condition changes during the drought period as well as the recovery of photosynthesis after rewatering. The SSiB2 reproduces reasonable simulations compared to remotely sensed observations, and the SIF modeling can be improved by constraining the parameterization with more observations. This study improves our understanding of using SIF observations to investigate the impacts of different water conditions on terrestrial ecosystems, as well as evaluating and improving model performance in SIF simulations.

#### Declaration of Competing Interest

The authors declare that they have no known competing financial interests or personal relationships that could have appeared to influence the work reported in this paper.

#### Acknowledgments

This research is financially supported by the National Key Research and Development Program of China (2017YFA0603803), the National Natural Science Foundation of China (grant no. 42175136), the Fundamental Research Funds for the Central Universities (grant nos. 14380059 and 14380172), and the Yunnan Natural Science Foundation of Yunnan Province, China (grant no. 2019IB018).

#### Appendix A. Supplementary material

Supplementary data to this article can be found online at <https://doi.org/10.1016/j.jag.2022.102832>.

#### References

- Beillouin, D., Schauburger, B., Bastos, A., Ciaï, P., Makowski, D., 2020. Impact of extreme weather conditions on European crop production in 2018. *Philos Trans R Soc Lond B Biol Sci.* 375, 20190510.
- Chen, D., Wang, S., Cao, B., Cao, D., Leng, G., Li, H., Yin, L., Shan, L., Deng, X., 2016. Genotypic variation in growth and physiological response to drought stress and rewatering reveals the critical role of recovery in drought adaptation in maize seedlings. *Front. Plant Sci.* 6.
- De Kauwe, M.G., Medlyn, B.E., Pitman, A.J., Drake, J.E., Ukkola, A., Griebel, A., Pendall, E., Prober, S., Roderick, M., 2019. Examining the evidence for decoupling

- between photosynthesis and transpiration during heat extremes. *Biogeosciences* 16, 903–916.
- Didan, K., 2015. MOD13C2 MODIS/Terra Vegetation Indices Monthly L3 Global 0.05Deg CMG. NASA EOSDIS Land Processes DAAC V006. doi: 10.5067/MODIS/MOD13C2.006.
- Doelling, D.R., Sun, M., Le Trang, N., Nordeen, M.L., Haney, C.O., Keyes, D.F., Mlynarczyk, P.E., 2016. Advances in geostationary-derived longwave fluxes for the CERES synoptic (SYN1deg) product. *J. Atmos. Ocean. Technol.* 33, 503–521.
- Dorigo, W., Wagner, W., Albergel, C., Albrecht, F., Balsamo, G., Brocca, L., Chung, D., Ertl, M., Forkel, M., Gruber, A., 2017. ESA CCI Soil Moisture for improved Earth system understanding: State-of-the art and future directions. *Rem. Sens. Environ.* 203, 185–215.
- Efeoglu, B., Ekmekeci, Y., Cicek, N., 2009. Physiological responses of three maize cultivars to drought stress and recovery. *S. Afr. J. Bot.* 75, 34–42.
- Fei, X.H., Song, Q.H., Zhang, Y.P., Yu, G.R., Zhang, L.M., Sha, L.Q., Liu, Y.T., Xu, K., Chen, H., Wu, C.S., 2019. Patterns and controls of light use efficiency in four contrasting forest ecosystems in Yunnan, Southwest China. *J. Geophys. Res.-Biogeosci.* 124, 293–311.
- Frankenberg, C., Fisher, J.B., Worden, J., Badgley, G., Saatchi, S.S., Lee, J.-E., Toon, G.C., Butz, A., Jung, M., Kuze, A., Yokota, T., 2011. New global observations of the terrestrial carbon cycle from GOSAT: patterns of plant fluorescence with gross primary productivity. *Geophys. Res. Lett.* 38 (17).
- Friedlingstein, P., Jones, M.W., O'sullivan, M., Andrew, R.M., Hauck, J., Peters, G.P., Peters, W., Pongratz, J., Sitch, S., Queré, C.L., 2019. Global carbon budget 2019. *Earth Syst. Sci. Data* 11, 1783–1838.
- Guanter, L., Zhang, Y., Jung, M., Joiner, J., Voigt, M., Berry, J.A., Frankenberg, C., Huete, A.R., Zarco-Tejada, P., Lee, J.-E., 2014. Global and time-resolved monitoring of crop photosynthesis with chlorophyll fluorescence. *Porc. Natl. Acad. Sci. U.S.A.* 111, E1327–E1333.
- Han, L., Zhang, Q., Yao, Y., Li, Y., Jia, J., Wang, J., 2014. Characteristics and origins of drought disasters in Southwest China in nearly 60 years. *Acta Geogr. Sin.* 69, 632–639.
- Humphrey, V., Berg, A., Ciaia, P., Gentile, P., Jung, M., Reichstein, M., Seneviratne, S.I., Frankenberg, C., 2021. Soil moisture–atmosphere feedback dominates land carbon uptake variability. *Nature* 592, 65–69.
- Jiao, W., Chang, Q., Wang, L., 2019. The sensitivity of satellite solar-induced chlorophyll fluorescence to meteorological drought. *Earth Future* 7, 558–573.
- Köhler, P., Frankenberg, C., Magney, T.S., Guanter, L., Joiner, J., Landgraf, J., 2018. Global retrievals of solar-induced chlorophyll fluorescence with TROPOMI: first results and intersensor comparison to OCO-2. *Geophys. Res. Lett.* 45, 10456–10463.
- Lee, J.E., Berry, J.A., Van Der Tol, C.S., Yang, X., Guanter, L., Damm, A., Baker, I., Frankenberg, C., 2015. Simulations of chlorophyll fluorescence incorporated into the Community Land Model version 4. *Glob. Change Biol.* 21, 3469–3477.
- Li, X., Li, Y., Chen, A., Gao, M., Slette, L.J., Piao, S., 2019. The impact of the 2009/2010 drought on vegetation growth and terrestrial carbon balance in Southwest China. *Agric. For. Meteorol.* 269, 239–248.
- Li, Z., Zhang, Q., Li, J., Yang, X., Wu, Y., Zhang, Z., Wang, S., Wang, H., Zhang, Y., 2020. Solar-induced chlorophyll fluorescence and its link to canopy photosynthesis in maize from continuous ground measurements. *Remote Sens. Environ.* 236, 111420.
- Liang, S.L., Cheng, J., Jia, K., Jiang, B., Liu, Q., Xiao, Z.Q., Yao, Y.J., Yuan, W.P., Zhang, X.T., Zhao, X., Zhou, J., 2021. The Global Land Surface Satellite (GLASS) product suite. *Bull. Amer. Meteorol. Soc.* 102, E323–E337.
- Magney, T.S., Barnes, M.L., Yang, X.I., 2020. On the covariation of chlorophyll fluorescence and photosynthesis across scales. *Geophys. Res. Lett.* 47 (23) <https://doi.org/10.1029/2020GL091098>.
- Martini, D., Sakowska, K., Wohlfahrt, G., Pacheco-Labrador, J., van der Tol, C., Porcar-Castell, A., Magney, T.S., Carrara, A., Colombo, R., El-Madany, T.S., Gonzalez-Cascon, R., Martín, M.P., Julitta, T., Moreno, G., Rascher, U., Reichstein, M., Rossini, M., Migliavacca, M., 2022. Heatwave breaks down the linearity between sun-induced fluorescence and gross primary production. *New Phytol.* 233 (6), 2415–2428.
- Michael Gunson, A.E., 2020. OCO-2 Level 2 bias-corrected solar-induced fluorescence and other select fields from the IMAP-DOAS algorithm aggregated as daily files, Retrospective processing, Greenbelt, MD, USA, Goddard Earth Sciences Data and Information Services Center (GES DISC), V10r. <https://doi.org/10.5067/XO2LBBNP0010>.
- Muñoz Sabater, J., 2019. ERA5-Land hourly data from 1981 to present. Copernicus Climate Change Service (C3S) Climate Data Store (CDS). <https://doi.org/10.24381/cds.e2161bac>.
- Myneni, R., Knyazikhin, Y., Park, T., 2015. MOD15A2H MODIS/Terra Leaf Area Index/FPAR 8-Day L4 Global 500m SIN Grid. NASA EOSDIS Land Processes DAAC V006. <https://doi.org/10.5067/MODIS/MOD15A2H.006>.
- O'Neill, P.E., Chan, S., Njoku, E.G., Jackson, T., Bindlish, R., Chaubell, J., SMAP L3 Radiometer Global Daily 36 km EASE-Grid Soil Moisture., Boulder, Colorado USA. NASA National Snow and Ice Data Center Distributed Active Archive Center., Version 6. <https://doi.org/10.5067/EVYDQ32FNWTH>.
- Parazoo, N.C., Magney, T., Norton, A., Raczka, B., Bacour, C., Maignan, F., Baker, I., Zhang, Y.G., Qiu, B., Shi, M.J., Macbean, N., Bowling, D.R., Burns, S.P., Blanken, P. D., Stutz, J., Grossmann, K., Frankenberg, C., 2020. Wide discrepancies in the magnitude and direction of modeled solar-induced chlorophyll fluorescence in response to light conditions. *Biogeosciences* 17, 3733–3755.
- Piao, S., Fang, J., Ciaia, P., Peylin, P., Huang, Y., Sitch, S., Wang, T., 2009. The carbon balance of terrestrial ecosystems in China. *Nature* 458, 1009–1013.
- Qiu, B., Chen, J.M., Ju, W., Zhang, Q., Zhang, Y., 2019a. Simulating emission and scattering of solar-induced chlorophyll fluorescence at far-red band in global vegetation with different canopy structures. *Remote Sens. Environ.* 233, 111373. <https://doi.org/10.1016/j.rse.2019.111373>.
- Qiu, B., Ge, J., Guo, W., Pitman, A.J., Mu, M., 2020. Responses of Australian dryland vegetation to the 2019 heat wave at a subdaily scale. *Geophys. Res. Lett.* 47, e2019GL086569.
- Qiu, B., Li, W., Wang, X., Shang, L., Song, C., Guo, W., Zhang, Y., 2019b. Satellite-observed solar-induced chlorophyll fluorescence reveals higher sensitivity of alpine ecosystems to snow cover on the Tibetan Plateau. *Agric. For. Meteorol.* 271, 126–134.
- Qiu, B., Xue, Y., Fisher, J.B., Guo, W., Berry, J.A., Zhang, Y., 2018. Satellite chlorophyll fluorescence and soil moisture observations lead to advances in the predictive understanding of global terrestrial coupled carbon-water cycles. *Glob. Biogeochem. Cycle* 32 (3), 360–375.
- Smith, N.E., Kooijmans, L.M.J., Koren, G., Van Schaik, E., Van Der Woude, A.M., Wanders, N., Ramonet, M., Xueref-Remy, I., Siebicke, L., Manca, G., Brummer, C., Baker, I.T., Haynes, K.D., Luijkx, I.T., Peters, W., 2020. Spring enhancement and summer reduction in carbon uptake during the 2018 drought in northwestern Europe. *Philos. Trans. R. Soc. B-Biol. Sci.* 375, 20190509.
- Song, L., Guanter, L., Guan, K., You, L., Huete, A., Ju, W., Zhang, Y., 2018. Satellite sun-induced chlorophyll fluorescence detects early response of winter wheat to heat stress in the Indian Indo-Gangetic Plains. *Glob. Change Biol.* 24 (9), 4023–4037.
- Stocker, T., 2014. Climate change 2013: the physical science basis: Working Group I contribution to the Fifth assessment report of the Intergovernmental Panel on Climate Change, Cambridge University Press.
- Sun, Y., Frankenberg, C., Jung, M., Joiner, J., Guanter, L., Köhler, P., Magney, T., 2018. Overview of Solar-Induced Chlorophyll Fluorescence (SIF) from the Orbiting Carbon Observatory-2: retrieval, cross-mission comparison, and global monitoring for GPP. *Remote Sens. Environ.* 209, 808–823.
- Wang, J., Feng, L., Palmer, P. I., Liu, Y., Fang, S., Bosch, H., O'dell, C. W., Tang, X., Yang, D., Liu, L. & Xia, C. 2020. Large Chinese land carbon sink estimated from atmospheric carbon dioxide data. *Nature* 586, 720–723.
- Wang, X., Qiu, B.o., Li, W., Zhang, Q., 2019. Impacts of drought and heatwave on the terrestrial ecosystem in China as revealed by satellite solar-induced chlorophyll fluorescence. *Scienceof. Total Environ.* 693, 133627. <https://doi.org/10.1016/j.scitotenv.2019.133627>.
- Yang, X., Tang, J., Mustard, J.F., Lee, J.E., Rossini, M., Joiner, J., Munger, J.W., Kornfeld, A., Richardson, A.D., 2015. Solar-induced chlorophyll fluorescence that correlates with canopy photosynthesis on diurnal and seasonal scales in a temperate deciduous forest. *Geophys. Res. Lett.* 42, 2977–2987.
- Yoshida, Y., Joiner, J., Tucker, C., Berry, J., Lee, J.-E., Walker, G., Reichle, R., Koster, R., Lyapustin, A., Wang, Y., 2015. The 2010 Russian drought impact on satellite measurements of solar-induced chlorophyll fluorescence: Insights from modeling and comparisons with parameters derived from satellite reflectances. *Rem. Sens. Environ.* 166, 163–177.
- Zhan, X.W., Xue, Y.K., Collatz, G.J., 2003. An analytical approach for estimating CO2 and heat fluxes over the Amazonian region. *Ecol. Model.* 162, 97–117.
- Zhong, S., Xu, Y., Meng, B.o., Loik, M.E., Ma, J.-Y., Sun, W., 2019. Nitrogen addition increases the sensitivity of photosynthesis to drought and re-watering differentially in C3 versus C4 grass species. *Front. Plant Sci.* 10 <https://doi.org/10.3389/fpls.2019.00815>.